

# Stability of two-dimensional, controlled, Bose-Einstein coherent states<sup>\*</sup>

D. Jovanović<sup>1,a</sup> and R. Fedele<sup>2</sup>

<sup>1</sup> Institute of Physics, P.O. Box 57, 11001 Belgrade, Serbia

<sup>2</sup> Dipartimento di Scienze Fisiche, Università Federico II and INFN Sezione di Napoli, Complesso Universitario di M.S. Angelo, via Cintia, 80126 Napoli, Italy

Received 9 October 2007 / Received in final form 9 November 2007

Published online 22 December 2007 – © EDP Sciences, Società Italiana di Fisica, Springer-Verlag 2007

**Abstract.** Two-dimensional stability of a controlled Bose-Einstein condensation state, in the form of a nonlinear Schrödinger soliton [JETP Lett. **80** 535 (2004)], is studied for the condensations with both repulsive and attractive inter-atom interactions. The Gross-Pitaevski equation is solved numerically, taking initially a controlled soliton whose “effective mass” is several times bigger than the critical value for a weak collapse in the absence of a potential well, and allowing for reasonably large errors in the experimental realization of the trapping potential required by the theory. For repulsive and sufficiently weak attractive interactions, the controlled state is shown to remain stable inside a breathing potential well, for a time that is an order of magnitude longer than the characteristic periods of the forced and eigenoscillations of the soliton. The collapse is observed only for attractive interactions, when the nonlinear attraction exceeded the appropriate threshold.

**PACS.** 03.75.Lm Tunneling, Josephson effect, Bose-Einstein condensates in periodic potentials, solitons, vortices, and topological excitations – 05.45.Yv Solitons – 05.30.Jp Boson systems

In the gas of identical bosons, particles may stimulate each other to occupy the lowest energy state, leading to a phase transition known as the Bose-Einstein condensation (BEC). It gives rise to a *macroscopic quantum-mechanical state* [1–3], described by a macroscopic quantum wavefunction. First, the BEC states were realized with mutually repelling atoms, e.g. <sup>87</sup>Rb, <sup>23</sup>Na, <sup>7</sup>Li, using advanced trapping techniques, such as the laser cooling in combination with magnetic evaporative cooling (for alkali atoms), and the evaporative cooling (for hydrogen) [4,5]. More recently, BEC states with the attracting interaction between atoms were also achieved, in the form of trains of one-dimensional (1-D) bright solitons, using all-optical traps, and controlling the interactions between the atoms by an oscillating magnetic field, via the Feshbach resonance [6,7]. It has been suggested that stable attractive 2-D and 3-D BEC solitons are also possible. A 2-D analytic theory based on the variational approximation, [8], together with 2-D and 3-D numerical simulations [9], predicted that they might be created in the periodic external potential of an optical lattice, while [10,11] suggested that the collapse of 2-D BEC solitons could be prevented also by parabolic potentials.

Existing technologies allow the design of an almost arbitrary potential well for a BEC experiment. Such are the lithographically fabricated circuit patterns, that provide electromagnetic guides and microtraps for ultracold systems of neutral atoms [12,13]. Even more “exotic” shapes of traps are achieved by the use of optically induced potentials [14]. Such versatility of the traps enables the production of a desired BEC spatial profile, by appropriately adjusting the potential well. In a recent paper, [15], a method was proposed for the filtering and control of stationary soliton-like states associated with the longitudinal dynamics of BECs, by controlling only a few external parameters. It was demonstrated that for an almost arbitrary a priori choice of the desired parameters of the solution, which belonged to the family of exact 1-D nonlinear Schrödinger solitons in the parallel direction and appropriately modulated in the perpendicular direction, one could self-consistently determine the necessary trapping potential. The nonlinear stability of such controlled BEC states was studied numerically [16] in a purely longitudinal, one-dimensional (1-D) case, but their perpendicular stability remained an open issue.

In this paper, we study the stability of a controlled BEC state in two dimensions. The Gross-Pitaevski equation is solved numerically, allowing for reasonably large (typically ~10%) errors in the experimental realization of the ideal trapping potential, predicted by theory. We

<sup>\*</sup> Online Material is available at <http://www.epj.org>

<sup>a</sup> e-mail: [djovanov@phy.bg.ac.yu](mailto:djovanov@phy.bg.ac.yu)

consider BECs with both repulsive and attractive inter-atom interactions, and controlled states whose effective mass exceeds the critical mass for a 2-D collapse of NLS solitons without an external potential. Two modes of oscillations, with similar characteristic frequencies, are detected – the eigenoscillations of a soliton that was initially displaced from the center of the well and the forced oscillations due to the “breathing”. For repulsive and sufficiently weak attractive interactions, the controlled state remains stable for at least ten periods of oscillations.

The Gross-Pitaevski (GP) equation

$$(i\partial_t + \nabla^2 + \beta|\psi|^2)\psi = v\psi, \quad (1)$$

arises frequently in physics, usually as an asymptotic approximation to a slowly varying wave envelope in the presence of an external potential. It is important for the studies in nonlinear optics, plasma physics, Bose-Einstein condensate, water waves, etc. The BEC is *weakly interacting* when  $|\beta| = \mathcal{O}(1)$ , with  $\beta < 0$  ( $\beta > 0$ ) corresponding to the repulsive (attractive) inter-atom interactions. Here  $\psi$  and  $v$  are the normalized wave function and the external potential, respectively. The latter depends explicitly on spatial and temporal coordinates.

Equation (1) has a number of interesting properties, the most important being that it can be integrated in some important special cases. For example, in the 1-D limit

$$\left[ i\partial_t + \partial_{z,z} + \beta|\psi(z,t)|^2 \right] \psi(z,t) = v(z)\psi(z,t), \quad (2)$$

it is completely integrable if the potential function,  $v(z)$ , is equal to zero. For  $\beta = 2$ , it reduces to the standard nonlinear Schrödinger (NLS) equation

$$\left[ i\partial_t + \partial_{z,z} + 2|\Psi_{\parallel}|^2 \right] \Psi_{\parallel} = 0. \quad (3)$$

The solution of equation (3), for an arbitrary initial condition, is the ensemble of solitons, immersed in the ‘bath’ of radiation. A soliton is determined by two free parameters,  $a$  and  $b$ , and has the form

$$\Psi_{\parallel}(a, b, z, t) = a e^{i[(a^2 - b^2)t + bz]} \operatorname{sech}[a(z - 2bt)]. \quad (4)$$

Now, we seek a solution of a more general 1-D GP equation, with  $v(z) \neq 0$ . A simple coherent structure can be constructed for a limited class of external potentials  $v(z)$ , if we require that the soliton  $\Psi_{\parallel}(a, b, z, t)$  satisfies also the Gross-Pitaevski equation (2), i.e. that  $\psi(z, t) = \Psi_{\parallel}(a, b, z, t)$ . Subtracting the above GP and NLS equations, we obtain that this is possible if the external potential  $v(z)$  is given by

$$v(z) = V(a, z) \equiv (\beta - 2)|\Psi_{\parallel}(a, 0, z, t)|^2. \quad (5)$$

In the above, we adopted  $b = 0$ , in order to have an external potential  $v$  that is independent on time. Conversely, adopting different values for the parameter  $a$  in the external potential, we can produce the solution of a 1-D GP equation with desired amplitude and spatial extend. Such solution we refer to as being *controlled*.

The question arises whether it is possible to control the solutions of the GP equation also in more realistic geometries, such as in 2-D and 3-D traps, and under which conditions such solution can be stable. For a two-dimensional Gross-Pitaevski (GP) equation

$$\left[ i\partial_t + \partial_{x,x} + \partial_{z,z} + \beta|\psi(x, z, t)|^2 \right] \psi(x, z, t) = v(x, z)\psi(x, z, t), \quad (6)$$

we seek the solution in the form

$$\psi(x, z, t) = \psi_{\perp}(x, t)\psi_{\parallel}(x, z, t), \quad (7)$$

where the function  $\psi_{\perp}(x, t)$  satisfies a linear 1-D Schrödinger equation, viz.

$$(i\partial_t + \partial_{x,x})\psi_{\perp}(x, t) = v_{\perp}(x, t)\psi_{\perp}(x, t). \quad (8)$$

Then, the longitudinal wave function  $\psi_{\parallel}(x, z, t)$  satisfies the following equation

$$\left[ i\partial_t + \partial_{x,x} + \partial_{z,z} + 2\frac{\partial_x\psi_{\perp}(x, t)}{\psi_{\perp}(x, t)}\partial_x + \beta|\psi_{\perp}(x, t)|^2|\psi_{\parallel}(x, z, t)|^2 \right] \psi_{\parallel}(x, z, t) = v_{\parallel}(x, z, t)\psi_{\parallel}(x, z, t), \quad (9)$$

where  $v_{\parallel}(x, z, t) = v(x, z, t) - v_{\perp}(x, t)$ . Without the loss of generality, we adopt a stationary and parabolic perpendicular controlling potential  $v_{\perp}(x, t) = x^2/2$ , i.e. we take that the 1-D equation (8) describes a linear oscillator. Its general solution is readily available in terms of normalized Hermite-Gauss modes, that constitute a complete set, viz.

$$\psi_{\perp}(x, t) = \Psi_{\perp}(x, t, \sigma_0, \gamma_0, k) \equiv \sum_{k=0}^{\infty} \alpha_k \left[ \pi 2^{2k+1} (k!)^2 \sigma(t)^2 \right]^{-\frac{1}{4}} \times \exp \left[ i\gamma(t) \frac{x^2}{4} - \frac{x^2}{4\sigma(t)^2} + i\phi(t) \right] H_k \left[ \frac{x}{\sqrt{2}\sigma(t)} \right]. \quad (10)$$

Here  $\alpha_k$  is the arbitrary amplitude of the  $k$ -th mode,  $H_k$  is a Hermite polynomial of the order  $k$ , the functions  $\sigma$ ,  $\gamma$  and  $\phi$  are given by

$$\sigma(t) = \frac{1}{\sqrt{2}\sigma_0} \times \sqrt{1 + \gamma_0^2 \sigma_0^4 + 2\gamma_0 \sin(2t)\sigma_0^4 + \sigma_0^4 - [(\gamma_0^2 - 1)\sigma_0^4 + 1] \cos(2t)} \quad (11)$$

$$\gamma(t) = \frac{4\gamma_0 \cos(2t)\sigma_0^4 + 2[(\gamma_0^2 - 1)\sigma_0^4 + 1] \sin(2t)}{2\{1 + \gamma_0^2 \sigma_0^4 + 2\gamma_0 \sin(2t)\sigma_0^4 + \sigma_0^4 - [(\gamma_0^2 - 1)\sigma_0^4 + 1] \cos(2t)\}} \quad (12)$$

$$\phi(t) = -\frac{1}{2}(2k+1) \cot^{-1} [\sigma_0^2(\gamma_0 + \cot(t))], \quad (13)$$

and  $\gamma_0$  and  $\sigma_0$  are the initial values  $\gamma_0 = \gamma(0)$  and  $\sigma_0 = \sigma(0)$ . It is instructive to present some simple special cases of the solution for the linear oscillator, equation (10), and a more extensive discussion is presented in reference [16].

- In the simplest case,  $\gamma_0 = 0$ ,  $\sigma_0 = 1$ , we have

$$\sigma(t) = 1, \quad \gamma(t) = 0, \quad \phi(t) = -\frac{1}{2}(2k+1) \quad (14)$$

and the perpendicular solution reduces to a time-stationary Hermite-Gauss function

$$\psi_{\perp}(x, t) = \sum_{k=0}^{\infty} \alpha_k \frac{\exp\left\{\frac{1}{4}[-x^2 - 2i(2k+1)]\right\}}{\sqrt{\pi 2^{2k+1} (k!)^2}} H_k\left(\frac{x}{\sqrt{2}}\right). \quad (15)$$

- For  $\gamma_0 = 0$ ,  $\sigma_0 \neq 1$ , we have

$$\sigma(t) = \frac{1}{\sqrt{2}\sigma_0} \sqrt{1 + \sigma_0^4 + (\sigma_0^4 - 1) \cos(2t)} \quad (16)$$

$$\gamma(t) = \frac{(1 - \sigma_0^4) \sin(2t)}{1 + \sigma_0^4 + (\sigma_0^4 - 1) \cos(2t)} \quad (17)$$

$$\phi(t) = -\frac{1}{2}(2k+1) \cot^{-1} [\sigma_0^2 \cot(t)]. \quad (18)$$

- For  $\gamma_0 \neq 0$ ,  $\sigma_0 = 1$ , we have

$$\sigma(t) = \frac{1}{\sqrt{2}} \sqrt{2 - \cos(2t) \gamma_0^2 + \gamma_0^2 + 2 \sin(2t) \gamma_0} \quad (19)$$

$$\gamma(t) = \frac{\gamma_0(2 \cos(2t) + \gamma_0 \sin(2t))}{2 - \cos(2t) \gamma_0^2 + \gamma_0^2 + 2 \sin(2t) \gamma_0} \quad (20)$$

$$\phi(t) = -\frac{1}{2}(2k+1) \cot^{-1} [\gamma_0 + \cot(t)]. \quad (21)$$

Obviously, expressions (16)–(18) and (19)–(21), after a substitution into equation (10), give Hermite-Gauss functions that are periodic in time, with the period  $\pi$ . As shown in reference [16], such periodicity gives rise either to the oscillatory “breathers” in the transverse BEC probability density of matter waves,  $|\psi_{\perp}|^2$ , or to its motion as a rigid body in the form of Lissajous figures, or it exhibits a Schrödinger cat state.

We conveniently adopt a potential  $v_{\parallel}(x, z, t)$  with the following spatial dependence

$$v_{\parallel}(x, z, t) = V_{\parallel}(a, x, z, t) \equiv \left[ \beta |\Psi_{\perp}(x, t, \sigma_0, \gamma_0, k)|^2 - 2 \right] |\Psi_{\parallel}(a, 0, z, t)|^2 \quad (22)$$

where  $\Psi_{\parallel}$  and  $\Psi_{\perp}$  are given by equations (4) and (10). Then, our 2-D GP equation (6) reduces to

$$\left\{ i\partial_t + \partial_{x,x} + \partial_{z,z} + 2 \frac{\partial_x \psi_{\perp}(x, t)}{\psi_{\perp}(x, t)} \partial_x + 2 |\Psi_{\parallel}(a, 0, z, t)|^2 + \beta |\psi_{\perp}(x, t)|^2 \left[ |\psi_{\parallel}(x, z, t)|^2 - |\Psi_{\parallel}(a, 0, z, t)|^2 \right] \right\} \psi_{\parallel}(x, z, t) = 0, \quad (23)$$

which obviously possesses one 1-D particular solution ( $\partial_x = 0$ ) in the form of a NLS soliton

$$\psi_{\parallel}(x, z, t) = \Psi_{\parallel}(a, 0, z, t) \equiv a e^{ia^2 t} \text{sech}(az). \quad (24)$$

This solution was proposed in reference [15], and its properties were studied extensively in [16]. Similarly to the 1-D case, it can be regarded as being *controlled*, since its basic properties (amplitude, longitudinal and perpendicular spatial scales, etc.) are determined by the external potential  $v_{\parallel}$ . Tuning the parameters  $a$ ,  $\alpha_k$ ,  $\gamma_0$ , and  $\sigma_0$ , we can produce BEC states whose main features, the amplitude and the spatial extend, are prescribed in advance.

The theory [15] was based on the separation of parallel and perpendicular dynamics even in a nonlinear state, yielding the parallel solution in the form of a NLS soliton. However, in more than one spatial dimension and without the external potential, the slab NLS soliton (24), is unstable to perpendicular perturbations, which trigger its filamentation and collapse [17]. For reviews about the NLS collapse see [18,19]. More detailed analytic analyses revealed that a cylindrically symmetric solitary solution of the NLS equation (6), with  $\partial_{x,x} + \partial_{z,z} = (1/r)\partial_r + \partial_{r,r}$ ,  $r = (x^2 + z^2)^{\frac{1}{2}}$ , and  $\beta = 2$ , becomes unstable if its “mass” exceeds a critical value [20,21],

$$M \equiv \int_0^{\infty} 2r dr |\psi(r, t)|^2 > 5.84. \quad (25)$$

A rough estimate for the characteristic perpendicular spatial scale of filamentation of a slab soliton, equation (24), can be made taking that its characteristic “critical mass” is comparable to the above, viz.

$$L_{\perp} \sim \frac{5.84}{\int_{-\infty}^{\infty} |\psi_{\parallel}(x, z, 0)|^2 dz}. \quad (26)$$

It is necessary to check the 2-D stability of BEC solitons in the presence of a controlling potential. While the stability of 2-D BEC structures has been confirmed for a class of periodic [8,9] and parabolic [10,11] trapping potentials, the stability properties of the bell-shaped potential well with finite depth, prescribed above, is still unknown. Furthermore, under realistic experimental conditions, the controlling potential is always realized with a certain deviation from its ideal form, equation (22). The perturbation of equation (23), resulting from such deviation, depends

explicitly on the soliton phase, and may grow secularly on a long timescale. Then, an important question arises whether in the presence of small but finite deviations (or errors) of the trapping potential, the solution of the 2-D GP equation remains stable, i.e. if it remains close to the soliton, equation (24), or deviates from it, and in particular, whether such deviation grows with time and possibly results in the destruction of the soliton.

In the 1-D case,  $\partial_x \psi_{\parallel} = 0$ , equation (23) was extensively studied in reference [16]. Detailed numerical simulations revealed that the solution  $\psi_{\parallel}$  remained stable for a broad class of errors in the experimental realization of the controlling potential, including deviations of more than 10% in the width and depth of the longitudinal potential well, as well as the asymmetries of the potential well and of the initial position of the soliton. The solution remained confined inside a non-ideal controlling potential for a long time, exhibiting longitudinal oscillations. Only a small part (<10%) was lost due to “radiation”, while the most part of BEC remained stable and preserved its shape.

We proceed by looking into the 2-D stability properties of the solution (24). Without loss of generality, we adopt the external potential  $v_{\parallel}$  in equation (23) in the form

$$v_{\parallel}(x, z, t) = \delta v_{\perp}(x, t) + \left[ \beta |\psi_{\perp 1}(x, t)|^2 - 2 \right] |\psi_{\parallel 1}(z, t)|^2, \quad (27)$$

where  $\delta v_{\perp}(x, t)$  is the small deviation of the perpendicular potential from an exact parabolic dependence, and  $\psi_{\perp 1}$  and  $\psi_{\parallel 1}$  are functions that are close to, but not identical to the exact solutions  $\psi_{\perp}$  and  $\psi_{\parallel}$ , given by equations (10) and (24). To establish the stability of the solution, equation (24), it would be necessary to solve our basic equation (23) with (27), for arbitrary functions  $\delta v_{\perp}(x)$ ,  $\psi_{\perp 1}$ , and  $\psi_{\parallel 1}$ . That is impossible to do numerically, and we restrict ourselves to a more modest task with  $\delta v_{\perp} = 0$ , with  $\psi_{\perp 1}$  and  $\psi_{\parallel 1}$  having the same form as their ideal counterparts  $\psi_{\perp}$ , and  $\psi_{\parallel}$ , with slightly different parameters, viz.

$$\psi_{\parallel 1}(z, t) = \alpha_{\parallel} \Psi_{\parallel} \left( a, 0, \frac{z - \delta z}{\lambda_{\parallel}}, \frac{t}{\tau_{\parallel}} \right), \quad (28)$$

$$\psi_{\perp 1}(x, t) = \alpha_{\perp} \Psi_{\perp} \left( \frac{x - \delta x}{\lambda_{\perp}}, \frac{t}{\tau_{\perp}}, \sigma_1, \gamma_1, k \right). \quad (29)$$

The parameters  $\alpha_{\perp}$ ,  $\alpha_{\parallel}$ ,  $\lambda_{\perp}$ ,  $\lambda_{\parallel}$ ,  $\tau_{\perp}$ , and  $\tau_{\parallel}$  are assumed to be close (e.g. within a 10% margin) to unity,  $\sigma_1$  and  $\gamma_1$  are close to the desired initial values,  $\sigma_0$  and  $\gamma_0$ , that correspond to the ideal perpendicular solution, while the displacements  $\delta x$  and  $\delta z$  are small compared to the soliton size. We consider only the simplest perpendicular solution  $\psi_{\parallel}$ , which corresponds to the ground state of a linear oscillator, viz.

$$\psi_{\perp}(x, t) = C \exp(-it/2 - x^2/4), \quad (30)$$

i.e. to the Hermite-Gauss function with  $\alpha_k = 0$ , when  $k \neq 0$ ,  $\gamma_0 = 0$ , and  $\sigma_0 = 1$ .  $C$  is an arbitrary constant.

Equation (23) was solved numerically on a standard PC. We used the method of lines, with a finite difference discretization of the spatial variables  $x$  and  $z$ , with  $50 \times 20$  points. Such relatively small resolution was sufficient to study the BEC dynamics with times up to  $t_{max} = 30$ , i.e. for almost ten oscillations of the non-ideal potential  $\psi_{\perp 1}$ , and to detect the onset of possible instabilities<sup>1</sup>. Then, at  $t = 0$ , the controlled solution  $\psi \equiv \psi_{\parallel} \psi_{\perp}$  takes the simple form

$$\psi(x, z, 0) = a C \exp(-x^2/4) \operatorname{sech}(az). \quad (31)$$

First, we studied the case of a repulsive inter-atom interaction,  $\beta < 0$ . The controlled soliton solution remained remarkably robust during its temporal evolution. For relatively shallow perpendicular potentials, corresponding to  $aC \ll 1$ , only small amplitude forced oscillations were detected, associated with the “breathing” of the external potential  $v_{\parallel}(x, z, t)$ , equation (27), associated with the oscillations of the function  $\psi_{\perp 1}$ , equation (29). For stronger perpendicular dependence of  $v_{\parallel}(x, z, t)$ , i.e. when  $aC > 1$ , the oscillations of the solution were more pronounced, sometimes approaching 50% of the initial value. Besides the forced oscillations due to the breathing of the controlling potential, also the eigenoscillations were observed, if the soliton was initially displaced from the center of the well. The characteristic frequencies of both types of oscillations were comparable. The oscillations were accompanied with relatively small emission of the soliton “mass”, both in the parallel and perpendicular directions (but due to the applied periodic boundary condition, the emitted mass would reenter the soliton on the opposite side). The effective mass of the soliton exceeded several times the critical mass for a weak, or 2-D, collapse of nonlinear Schrödinger solitons in the absence of an external potential, but the collapse/filamentation instability was not observed. Even the accumulation of the numerical error (noticeable as the striation of the solution, with the scalelength commensurable with the step size of the grid in the  $x$  direction) did not trigger any filamentation. The calculation was terminated around  $t = 27$ , due to the build up of numerical errors. Similar results were obtained also for weak attractive interactions,  $\beta = 0.15$ , featuring only slightly larger forced oscillations of the soliton amplitude. For strong attractive interactions,  $\beta = 1$ , a collapse/filamentation occurred during the time shorter than the period of oscillations. For intermediate attractive potentials,  $0.15 \lesssim \beta \lesssim 1$ , soliton oscillations with growing amplitudes were observed, but due to the rapid accumulation of numerical error we were not able to follow the full dynamics and to determine the exact threshold (in  $\beta$ ) for the collapse.

Typical results are displayed in Figure 1. These plots were obtained with the following choice of the parameters  $a = 1.5$ ,  $C = 1.58$ ,  $k = 0$ ,  $\gamma_0 = 0$ ,  $\sigma_0 = 1$ ,  $\gamma_1 = 0.05$ ,  $\sigma_1 = 0.95$ ,  $\alpha_{\perp} = 0.9$ ,  $\alpha_{\parallel} = 1.15$ ,  $\lambda_{\perp} = 0.9$ ,  $\lambda_{\parallel} = 1.2$ ,  $\tau_{\perp} = 1.15$ ,  $\tau_{\parallel} = 1.3$ , with  $\beta = -1$ ,  $\beta = 0.15$ , and  $\beta = 1$ . The initial displacements of the soliton from the center of the

<sup>1</sup> This was tested by solving a 2-D NLS equation by the same code, yielding a filamentation instability with the spatial period close to the predicted length, equation (26).

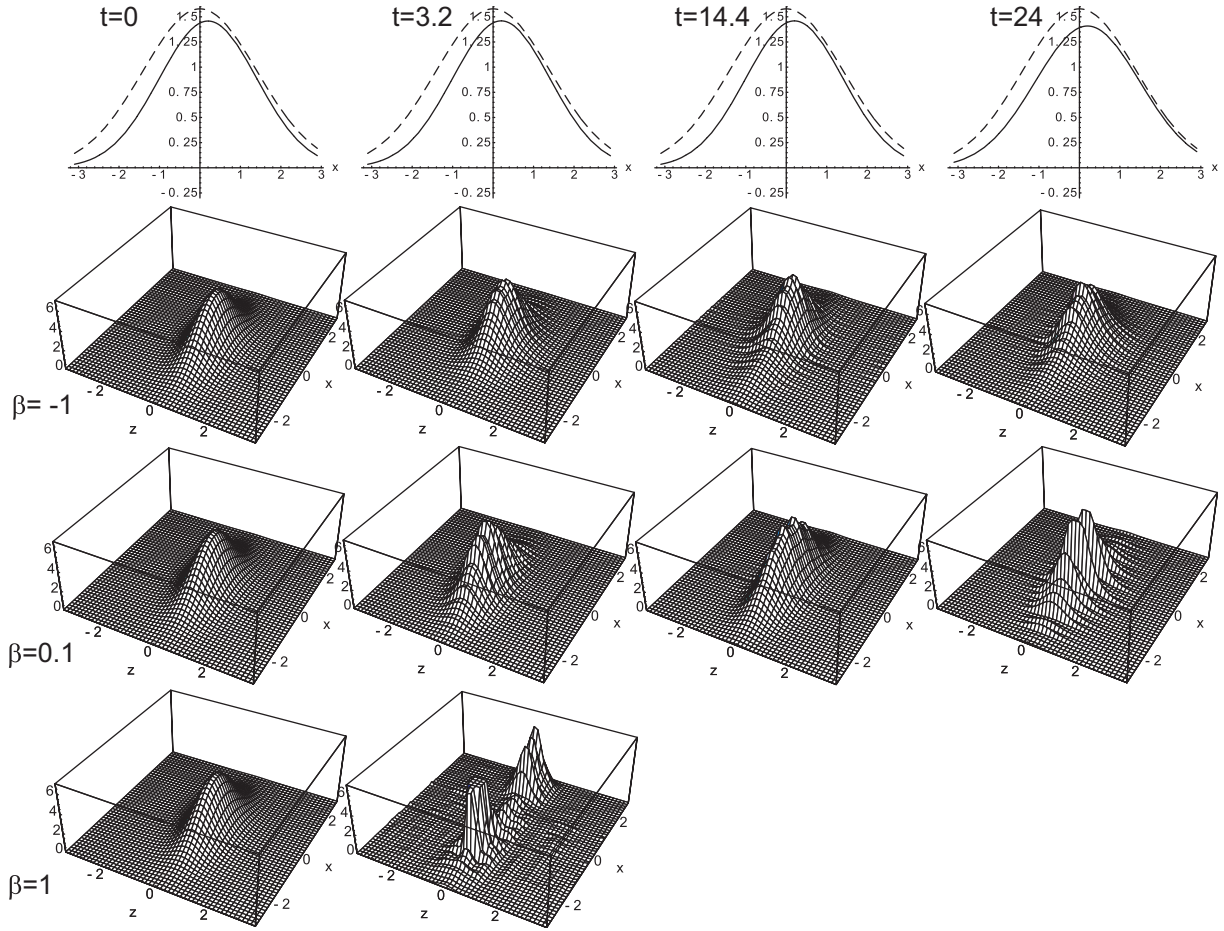


**Fig. 1.** Temporal dependence of the wavefunction. For the times indicated in the figure, from top to bottom are shown the perpendicular wavefunctions,  $|\psi_{\perp}|^2$  and  $|\psi_{\perp 1}|^2$  (dashed and solid lines, respectively, plots in the first row), and the complete wavefunction  $|\psi|$ , for repulsive interactions ( $\beta = -1$ , second row), weak attractive interactions ( $\beta = +0.15$ , third row) and stronger attractive interactions ( $\beta = +1$ , fourth row). The parameters are adopted as  $a = 1.5$ ,  $C = 1.58$ ,  $k = 0$ ,  $\gamma_0 = 0$ ,  $\sigma_0 = 1$ ,  $\gamma_1 = 0.05$ ,  $\sigma_1 = 0.95$ ,  $\alpha_{\perp} = 0.9$ ,  $\alpha_{\parallel} = 1.15$ ,  $\lambda_{\perp} = 0.9$ ,  $\lambda_{\parallel} = 1.2$ ,  $\tau_{\perp} = 1.15$ , and  $\tau_{\parallel} = 1.3$ . These plots are still frames, extracted from the animations that are given in the “Online Material”.

potential well were  $\delta x = 0.2$  and  $\delta z = 0.25$ . The critical length for filamentation of NLS solitons, equation (26), is estimated as  $L_{\perp} = 1.23$ , which is roughly 40% of the width (in the  $x$  direction) of the controlled GP soliton, equation (31). This is consistent with the results in the unstable, i.e. sufficiently strong attractive case, when a collapse into two filaments was observed.

The first row of Figure 1. shows the temporal dependence of the intensities of the perpendicular wavefunctions,  $|\psi_{\perp}|^2$  and  $|\psi_{\perp 1}|^2$  (dashed and solid lines, respectively). The temporal evolution of the potential  $|\psi|$  is displayed in the rows 2-4, for the cases of the repulsive inter-atom interactions,  $\beta = -1$ , weak attractive interactions  $\beta = +0.15$  and stronger attractive interactions,  $\beta = +1$ , respectively.

In conclusion, we have performed a systematic stability study of a controlled BEC state in two dimensions. A 2-D Gross-Pitaevski equation, for a weakly interacting condensation with repelling inter-atom interactions, was solved numerically, allowing for reasonably large (typically

$\sim 10\%$ ) errors in the experimental realization of the ideal trapping potential, and for a broad range of soliton parameters. Errors in the controlling potential that are associated with its “forced breathing”, produce the forced oscillations of the soliton, while the asymmetries of the soliton initial position inside the well lead to its eigenoscillations. The characteristic frequencies of these oscillations are of similar order. We considered BECs with both repulsive and attractive inter-atom interactions, and controlled solitons whose effective mass exceeded the critical mass for a weak, or 2-D, collapse of nonlinear Schrödinger solitons in the absence of a potential trap. For repulsive and sufficiently weak attractive interactions, the collapse/filamentation instability was not observed, while for stronger attractive interactions the collapse occurred within a finite time, shorter than the period of soliton oscillations. A better spatial resolution might be necessary to follow the soliton evolution for longer times, which would reveal the exact value of the threshold and the time of collapse, in the case of intermediate strengths of

repulsive interactions. In the case of stable oscillations (for repulsive or weak attractive interactions), it would be interesting to check if a resonance between its forced and eigenoscillations, which can be made possible by the appropriate choice of the width and depth of the potential well, leads to the growing oscillations and the destruction of the BEC state.

## References

1. S.N. Bose, *Zeitschrift Phys.* **26**, 178 (1924)
2. A. Einstein, *Sitzungsberichte der Preussischen Akademie der Wissenschaften* (1924)
3. M.A. Anderson, B.P. Kasevich, *Science* **282**, 1686 (1998)
4. K. Burnett, *Contemp. Phys.* **37**, 1 (1996)
5. A.J. Leggett, *Rev. Mod. Phys.* **73**, 307 (2001)
6. L. Khaykovich et al., *Science* **296**, 1290 (2002)
7. K.E. Strecker et al., *Nature* **417**, 150 (2002)
8. B.B. Baizakov et al., *Europhys. Lett.* **63**, 642 (2003)
9. D. Mihalache et al., *Phys. Rev. A* **72**, 021601 (2005)
10. B. Lemesurier, P. Christiansen, *Phys. D* **184**, 226 (2003)
11. B.J. Lemesurier et al., *Phys. Rev. E* **70**, 046614 (2004)
12. J. Reichel, *App. Phys. B* **74**, 469 (2002)
13. R. Folman et al., *Adv. At. Mol. Opt. Phys.* **48**, 263 (2002)
14. R. Grimm et al., *Adv. At. Mol. Opt. Phys.* **42**, 95 (2000)
15. R. Fedele et al., *JETP Lett.* **80**, 535 (2004)
16. S. de Nicola et al., *Eur. Phys. J. B* **54**, 113 (2006)
17. S.N. Vlasov et al., *Radiophys. Quant. Electr.* **14**, 1062 (1971)
18. J.J. Rasmussen, K. Rypdal, *Phys. Scr.* **33**, 481 (1986)
19. P.A. Robinson, *Rev. Mod. Phys.* **69**, 507 (1997)
20. S.K. Turitsyn, *Phys. Rev. E* **47**, 13 (1993)
21. E.A. Kuznetsov et al., *Phys. D* **87**, 273 (1995)